PHYSICAL REVIEW B **91**, 041204(R) (2015)

Effectiveness of organic molecules for spin filtering in an organic spin valve: Reaction-induced spin polarization for Co atop Alq_3

Tu-Ngoc Lam,[1] Yu-Ling Lai,[2] Chih-Han Chen,[2] Po-Hung Chen,[3] Yuet-Loy Chan,[2] Der-Hsin Wei,[2] Hong-Ji Lin,[2] C. T. Chen,[2] Jeng-Han Wang,[4,*] Jeng-Tzong Sheu,[1,†] and Yao-Jane Hsu[2,‡]

[1]*Department of Materials Science and Engineering, National Chiao Tung University, Hsinchu 30010, Taiwan, Republic of China*

[2]*National Synchrotron Radiation Research Center, 101 Hsin-Ann Road, Hsinchu Science Park, Hsinchu 30076, Taiwan, Republic of China*

[3]*Department of Engineering and System Science, National Tsing Hua University, Hsinchu 30013, Taiwan, Republic of China*

[4]*Department of Chemistry, National Taiwan Normal University, Taipei 11677, Taiwan, Republic of China*

(Received 7 October 2013; revised manuscript received 3 December 2014; published 21 January 2015)

The spin polarization of organic-ferromagnetic interfaces in an organic spin valve critically affects the efficiency of spin injection or detection. We examined the chemical and electronic properties of ferromagnetic Co deposited on organic Alq_3 and the interfacial spin-polarized capability of the electronic states. Our x-ray photoemission spectra and calculations with density-functional theory indicate a sequential and unequal distribution of charge from Co clusters to N and then to O atoms in Alq_3. The preferential orbital hybridization at specific functional sites produces efficient spin polarization of organic molecules. Element-specific measurements of x-ray magnetic circular dichroism demonstrate the preferential spin polarization in the lowest unoccupied molecular orbital state of N atoms at the complex interface for Co atop Alq_3, which agrees satisfactorily with calculation. Our results indicate that an induced interfacial spin polarization on engineering the dominant reaction of Co with mainly N and O atoms in Alq_3 might pave a way for effective spin filtering in organic spintronics.

DOI: 10.1103/PhysRevB.91.041204 PACS number(s): 79.60.Fr, 75.70.Cn, 68.35.Fx, 75.76.+j

Organic spin valves (OSV) in which an organic semiconductor (OSC) spacer is sandwiched between two ferromagnetic (FM) electrodes have attracted much attention because of an enduring spin coherence of organic materials via weak spin-orbit coupling [1]. Dediu *et al.* pioneered in achieving magnetoresistance (MR) up to 30% near 295 K in a $La_{0.7}Sr_{0.3}MnO_3$(LSMO)/sexithiophene(T_6)/LSMO OSV, initiating a great potential of organic-based spintronics [2]. Xiong *et al.* subsequently made a remarkable observation of a giant MR at 40% at 11 K in a LSMO/Alq_3/Co OSV [1]. Among the most widely used OSC in OSV, tri(8-hydroxyquinoline) aluminum (Alq_3) composed of π-conjugated molecules is considered to be a promising material for effective spin transport because of its great spin-relaxation time and unique molecular structure [1,3–6]. The combination of Alq_3 and *d*-band FM Co has achieved striking MR values [1,7–12]. Although an ill-defined layer between Alq_3 and top Co was manifested at an Alq_3 thickness greater than 100 nm, it is one of few examples in which an OSV displayed a large MR [1]. Such an ill-defined layer is ascribed to the diffusion of metal into a soft organic layer, which might be related to the disputed results of the MR sign and mechanism [1,12–15]. To prevent the unexpected interdiffusion and chemical interaction at the interfacial region, a buffer layer inserted between the top Co and Alq_3 has improved the device performance [9,16–18]. Although metal interdiffusion is preventable with those methods, it might not provide a deep understanding of the lacking essential mechanisms [19–21]. Moreover, in the case of an OSV with no buffer layer, a large MR was still achieved [1,8]. Various techniques have been used to engineer, to control, or to detect the efficient spin injection and transport [1,4,22,23] on traditionally applying a specific bias voltage to inject spin-polarized carriers [1], or using spin-resolved two-photon photoemission to excite the spins across a FM-OSC heterojunction [23], or pumping spins through a FM resonance to inject spin currents [24]. Although many mechanisms and experiments have been tried, a clear picture of how effective carrier states near the Fermi level (E_F) generated from a hybridized interface for an efficient spin injection and transport is still lacking. A complicated spin injection and transport are governed by many parameters, such as barriers to the injection of holes or electrons, energy levels of transport by lowest unoccupied molecular orbital (LUMO) or highest occupied molecular orbital (HOMO), a space-charge-limited current, deep or shallow traps, the carrier mobility and charge transfer, and the interfacial spin polarization (SP) at the FM-OSC contact. Among those parameters, the spin dependence at the interface of organic adsorption on a FM substrate plays a significant role as spin-polarized charge carriers must cross these interfaces [25–33]. In addition, the interfacial SP is critical to determine the promising candidates as OSV, because most parameters have been generally considered in organic electronics. Zhan *et al.* demonstrated an induced SP through hybridization and exchange coupling at the interface of Alq_3 adsorbed on Fe [29]; Steil *et al.* discovered that the hybrid states at the interface of Alq_3 adsorbed on Co at which electrons are trapped act as spin filters [32]. The interfacial SP role at the top contact of a FM atop an OSC is, however, still unknown and more complicated because penetration, diffusion, and reaction of a metal occur at the ill-defined interface [13,34–36]. In the worst case, for a fragile OSC, the reaction might modify or damage the molecular structures and yield degraded electronic and magnetic properties [37]. Only a MR response is hence measured for fragile organic molecules in a planar-type OSV [38]. The situation might differ completely if the molecules contain an appropriate functional group that can resist degradation and become spin polarized. As the top FM in an OSV using Alq_3

*jenghan@ntnu.edu.tw
†jtsheu@faculty.nctu.edu.tw
‡yjhsu@nsrrc.org.tw

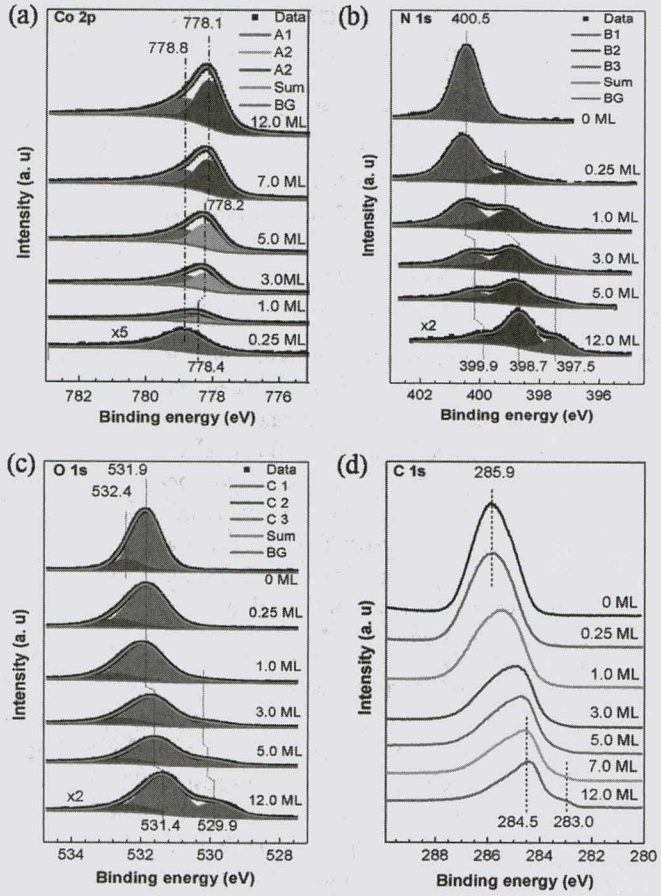

FIG. 1. (Color online) Core-level photoelectron spectra of varied Co thickness on Alq_3 in (a) Co $2p$, (b) N $1s$, (c) O $1s$, and (d) C $1s$ regions with incident photon energies 900, 480, 620, and 380 eV, respectively. The curve indicated with black square symbols (data), overlaps the sum curve of the spectrum (sum). Shirley background (BG) correction is used in deconvoluting XPS.

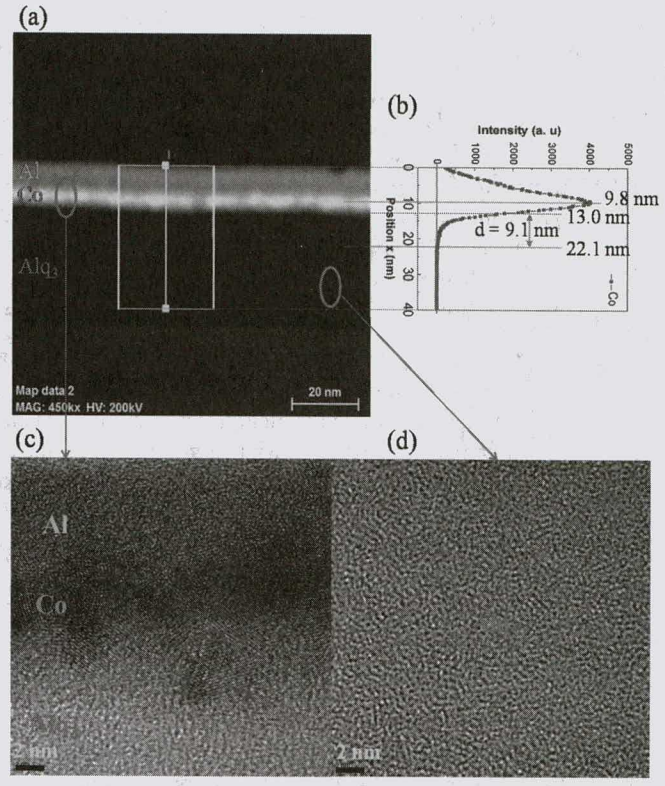

FIG. 2. (Color online) TEM/EELS at Alq_3-Co_{top} interface. (a) TEM image of 28.0 ML Co (thickness 5 nm) atop Alq_3 (thickness 30 nm), with an Al capping layer (thickness 8 nm). (b) Intensity profile of Co distribution corresponding to marked positions of Co diffused into Alq_3. TEM images of the magnified regions (c) near the Alq_3-Co_{top} interface and (d) for bulk Alq_3.

as a nonmagnetic spacer directly controls the performance of the device [9], we examined the electronic structures of the interfacial region and the SP of Alq_3-Co_{top} bilayers to seek the criteria of organic molecules effective for spintronics.

To understand the interplay between organic molecules and a FM metal, we examined the interfacial electronic properties of Co atop Alq_3 by x-ray photoelectron spectroscopy (XPS). At 0.25 ML Co atop Alq_3, the single line at binding energy (BE) 778.8 eV (A1) in Fig. 1(a), corresponds to Co hybridized with primary sites of Alq_3. After 1.0 ML Co deposition, a new line appeared towards smaller BE 778.4 eV (A2), indicating the formation of a more complicated hybridization of Co with sequential reactive sites of Alq_3. This feature became nearly unaltered at 778.1 eV when the Co thickness attained 7.0 ML, indicating the formation of a metallic Co film. A gradual shift from a large to a small BE with increasing Co coverage demonstrated the charge transfer from Co to Alq_3.

The N $1s$ line of bulk Alq_3 is located at BE 400.5 eV (B1) in Fig. 1(b). A new line near 398.7 eV was observed after deposition of a submonolayer of Co (B2), indicating that charge is initially donated from Co to N atoms. The new component of N $1s$ appeared at a small Co coverage and rose to a discrete maximum above 1.0 ML Co at which the induced extra charge on O atoms only began to occur. The original O $1s$ signal is seen at BE 531.9 eV [C1 in Fig. 1(c)], whereas the satellite line, measured at 532.4 eV, is attributed to $\pi \rightarrow \pi^*$ transitions (C2). Accompanying the shift of BE to smaller energy and the decreased intensity of the original O $1s$ signal, an additional line was detected at BE 529.9 eV (C3) in the monolayer range of Co. In contrast to having only one extra component at O $1s$, further Co deposition induced a second N $1s$ component at smaller BE 397.5 eV, described as B3 in Fig. 1(b). The energies of these N $1s$ lines are 1.8 and 3.0 eV, respectively, less than that of the original N $1s$ line after 5.0 ML Co deposition. Compared to the proposed strong interaction between Co and O atoms [11], our results indicate that both N and O atoms accept charge from Co, but, during the initial deposition of Co, the charge was donated preferentially to N atoms. Up to 7.0 ML Co deposition, the C $1s$ signal displayed as a broad feature at BE 283.0 eV, representing the formation of cobalt carbide [39], shown in Fig. 1(d).

To provide detailed information about the interfacial region of Co atop Alq_3, a cross-sectional view from a high-resolution transmission electron microscope (TEM) is shown in Fig. 2(a). The intensity of Co along the interfacial plane obtained in measurements of electron energy-loss spectroscopy (EELS) in Fig. 2(b) decreases slowly and is even visible over 9 nm towards Alq_3, demonstrating the penetration of a Co atom or clusters up to 9 nm into Alq_3. A clear distinction of molecular patterns and image contrast between the region

near the Alq_3–Co_{top} interface and deep bulk Alq_3 is observed in the cross-sectional TEM images in Figs. 2(c) and 2(d), respectively. The Co bunch roughly 2 nm in the frontier seemed to be diffused into Alq_3 and led to intermixed patterns. Although EELS indicated the existence of Co signals as deep as 9 nm, no resolvable nanometer-size particle was detected. This result implies that the sizes of most interdiffused Co clusters into Alq_3 were beyond the detection limit and might be in the range of several to several tenths of Co atoms.

As mentioned in the XPS results, a charge transfer from Co occurred first to N and then to other atoms. Calculation with density-functional theory (DFT) [40–43] was employed to examine the adsorption energy (E_{ads}) and the induced magnetization or SP of Alq_3 in the charge transfer and magnetic coupling with a Co atom (Alq_3-Co) and stable clusters (Alq_3-Co_4 and Alq_3-Co_2) that correlated satisfactorily with interdiffused Co cluster sizes obtained in TEM images. E_{ads} is defined as $E_{ads} = E(Alq_3\text{-}Co_x)\text{-}E(Alq_3)\text{-}E(Co_x)$, which are total energies of the Alq_3-Co_x complex, Alq_3, and the Co atom or clusters, respectively. SP is defined as $SP = [DOS(\alpha)\text{-}DOS(\beta)]/[DOS(\alpha) + DOS(\beta)]$, which are density of state (DOS) areas for spins α and β. The DOS areas were integrated from -1.0 eV to E_F and from E_F to 1.0 eV for SP analyses in the HOMO and LUMO states, respectively. The energetic result (E_{ads} are -3.4, -6.5, and -6.1 eV when Co, Co_2, and Co_4, respectively, bond to N of Alq_3, and are -2.8, -5.1, and -5.0 eV when Co, Co_2, and Co_4, respectively, bond to O of Alq_3) implies that a Co atom or Co clusters primarily attach to N atoms or rings and then to O atoms or rings, in agreement with our XPS observation. Additionally, those E_{ads} for Alq_3-Co_{top} complexes are much greater than E_{ads} (-1.0 eV) for Alq_3 on a Co (111) surface [44], indicating that a FM layer atop an OSC results in an enhanced FM-OSC interaction to shape Alq_3 for effective spin filtering. The SP analyses for the most stable Alq_3-Co_2 complex, in which Co_2 bonds between two pyridyl rings with $E_{ads} = -6.5$ eV, are shown in Fig. 3, for example. Figure 3(a) indicates an unbalanced spin density about 0.9 eV above E_F on the N site, but the DOS of O shows a disparity below E_F, as seen in Fig. 3(b). The cluster Co_2 in a hybridized complex maintains a much larger SP (majority on a spin-down channel near E_F), shown in Fig. 3(c). Accordingly, the distribution of spin-polarized charge density of the Alq_3-Co_2 complex in Fig. 3(d) shows that Alq_3 is spin-polarized on the LUMO of N (blue isosurfaces) and on the HOMO of O atoms (red isosurfaces). Another example of the Alq_3-Co_2 complex, in which Co_2 bonds between two phenoxide rings with $E_{ads} = -5.1$ eV, yields a similar result in Fig. 3(e). DFT calculations reveal that O and N atoms express inverse magnetization and SP, which illustrates a positive value for O but a negative value for N below E_F and vice versa above E_F, shown in Figs. 3(f) and 3(g). That condition might determine the dominant spin-polarized carriers at the Alq_3-Co_{top} interface, possibly affecting the MR sign that might be feasibly manipulated on tuning the alignment of energy levels between E_F, LUMO, and HOMO states for carrier injection. The magnetic moments of spin-polarized N atoms indicated in Fig. 3(a) are $-0.01\mu_B$ and $0.03\mu_B$ (even attaining $0.05\mu_B$ for Co_4 bonded with N and O), which are the same as, or about ten times, those of $-0.01\mu_B$ and $0.003\,\mu_B$ for the Fe_{bottom}-Alq_3 model [29]. Similarly, the calculated SP, 9%, for hybridized N and O in Alq_3-Co_{top} complexes is greater than that of the Fe_{bottom}-Alq_3 model [29], confirming that an enhanced FM-OSC interaction improves the spin filtering for a FM-OSC hybridized surface. The SP of an individual N or O atom can even attain 50%, but its SP polarity is not readily aligned in the same direction, resulting in a decreased SP of the entire Alq_3 molecule. Possibly designing the local SP of an individual N or O atom towards the same sign might effectively enhance the total SP of Alq_3. The SP of O atoms above E_F is too small to be detected experimentally with x-ray absorption spectra (XAS) or x-ray magnetic circular dichroism (XMCD) because of a small and symmetric spin-polarized DOS at the LUMO state; we thus employed element-specific XMCD to examine the SP of only N atoms. Verifying experimentally the SP of the O character at the HOMO state requires more sophisticated measurements, such as spin-resolved photoemission spectra [32].

Because the diffusion of Co into Alq_3 might attain a depth as great as 9 nm, measuring XMCD with sequential Co evaporation provides a depth-dependent SP that is crucial for effective spin filtering for an Alq_3-Co_{top} complex. A small XMCD of the Co L_3-edge [dichroic ratio (DR) ~0.4%, compared with DR ~15% of a 19.0 ML Co film) and the N K edge (DR ~0.2%) was observed at 3.5 ML Co, but no XMCD of the Co L_2 edge was detected, according to the inset of Fig. 4(a), implying that no significant long-range order was formed to create a FM ordering near 295 K. This result is ascribed to the exchange energy necessary to align the spins of diffused and hybridized Co nanoparticles being smaller than the thermal fluctuation that tends to diminish the weak magnetic dipole-dipole interactions produced by the individual spins. A retarded FM property of Co in doping with organic molecules was found [35–36]; an insufficiently metallic Co could hence be another reason to explain the suppression of magnetization found in the Co XMCD. To clarify the origin of the loss of ferromagnetism of Co near 295 K, we examined the FM properties of 3.5 ML Co on Alq_3 at 79 K. Through the Co XMCD for a sample cooled to 79 K, we observed a XMCD signal, displayed in Fig. 4(b). Because the metallic Co did not become dominant until its thickness attained 7.0 ML, what we observed represents a FM order originating mainly from a hybridized Co-Alq_3 complex. Up to 5.0 ML Co atop Alq_3 (DR at Co L_3 edge ~2.8%), a N XMCD more pronounced than that for a Fe_{bottom}-Alq_3 interface [29] with DR 0.6% was obtained in Fig. 4(c). This result demonstrates that Alq_3 hybridized with Co clusters within the ill-defined interface was highly magnetized and spin polarized, coinciding with our DFT calculation that shows an Alq_3-Co_{top} complex to be more effective for spin filtering. The FM ordering at 295 K began, however, to be established at 6.5 ML Co according to an appearance of a small but significant XMCD of the Co L_3 edge (DR ~1.2%), shown in the inset of Fig. 4(d). The presence of FM order was detected at 79 K, depicted in Fig. 4(e). At this Co coverage, the DR of the N character at the LUMO state was also prominently obtained with value 0.4%, presented in Fig. 4(f). The decreased temperature indicates, however, that the dominant species of the hybridized Alq_3-Co_{top} complex exhibited FM ordering that might explain the magnetic response found at 79 K. Figure 4(g) depicts the

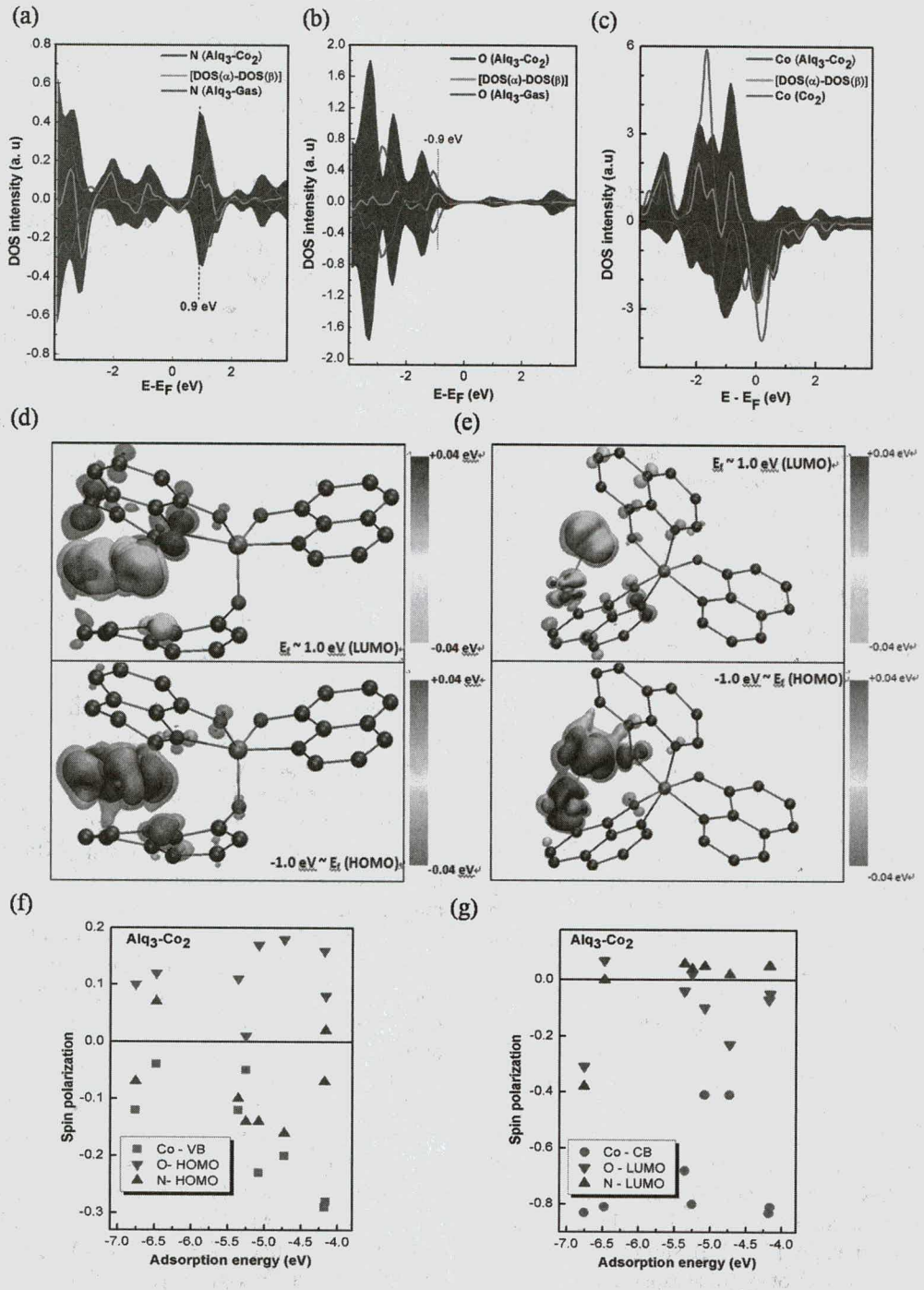

FIG. 3. (Color online) Spin-polarized partial DOS of N, O, and Co_2 cluster in (a), (b), and (c), respectively. Distributions of spin-polarized charge density of an Alq_3-Co_2 model in which Al, C, N, O, and Co atoms are shown as orange, black, blue, red, and yellow spheres, respectively. The blue and yellow isosurfaces are spin-up and spin-down charge densities, respectively, set to 0.04 $|e|$ /Å^3 at the LUMO state, whereas the red and orange isosurfaces are spin-up and spin-down charge densities, respectively, set to 0.04 $|e|$ /Å^3, at the HOMO state, for a Co_2 cluster bonded with two pyridyl rings (d) and phenoxide rings (e). SP of Co, O, and N atoms at the HOMO (f) and LUMO states (g).

preferential spin-polarized trend of constituent atoms in Alq_3 at the interfacial Alq_3-Co_{top} region. The spin-polarized N orbitals are induced by not only the adsorption of Alq_3 on FM substrate in the well-defined interface but also the FM layer atop Alq_3 in the ill-defined interface, making Alq_3 a unique and dominant organic substance for spin filtering in OSV.

In summary, we demonstrated a strongly reactive interface of Co atop Alq_3 in which N atoms of pyridyl rings served as primary reactive sites and O atoms of phenoxide rings were secondary reactive sites. The Alq_3-Co_{top} interface played a role as spin filter in which the induced SP of Alq_3 came mainly from the SP of N orbitals at the LUMO state and O orbitals at the HOMO state. Our results indicate that, if engineering of the spin interface can manipulate the reaction of a FM metal with specific functional sites of organic molecules so as to induce more effective SP, it could pave a way for a highly efficient SP in the manufacture and operation of real OSC-FM hybrid-based OSV.

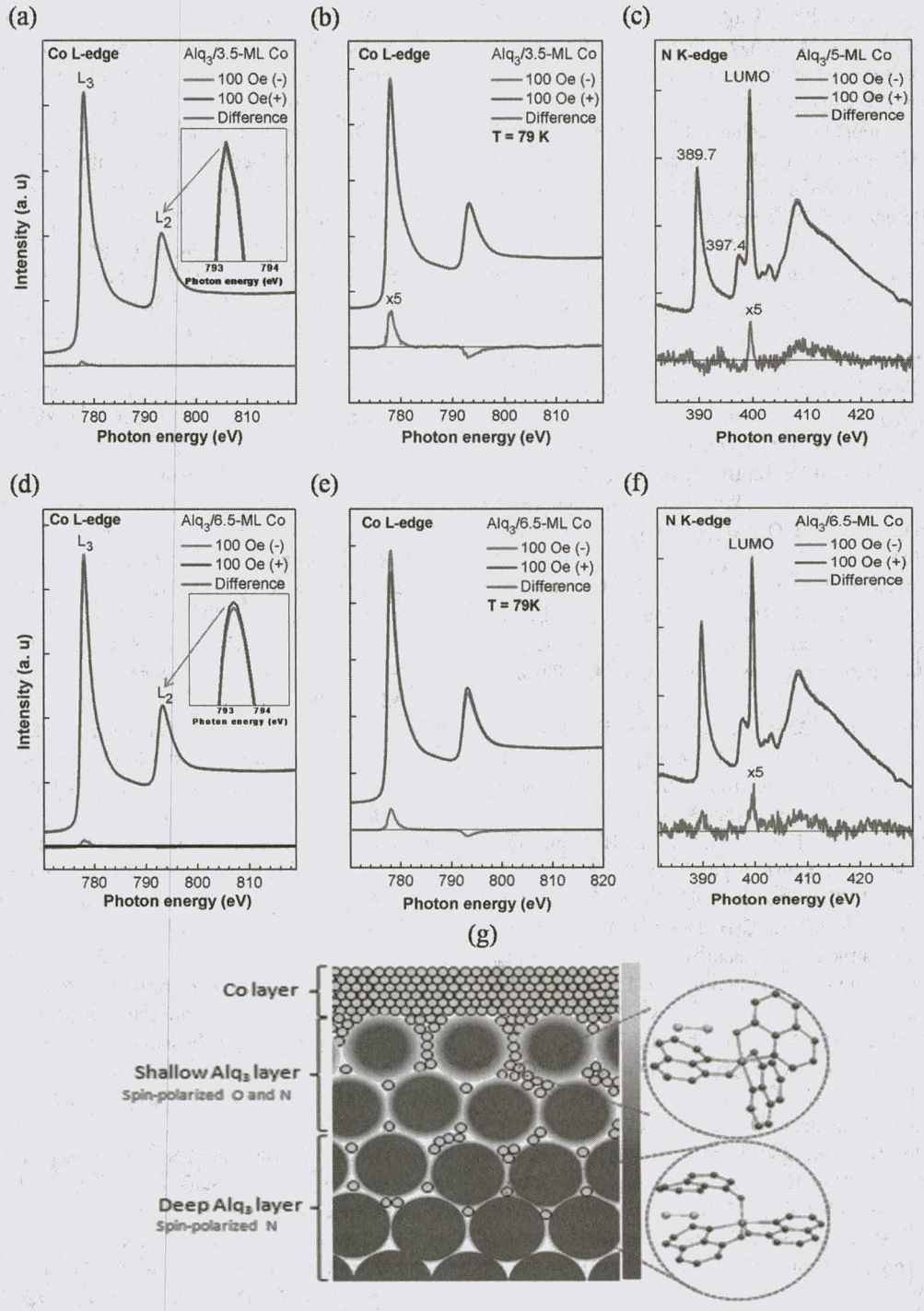

FIG. 4. (Color online) Magnetic properties of Co atop Alq_3. Co *L*-edge XAS/XMCD (a) near 295 K and (b) at 79 K for 3.5 ML Co. (c) N *K*-edge XAS/XMCD for 5 ML Co. Co XMCD (d) near 295 K and (e) at 79 K for 6.5 ML Co. (f) N *K*-edge XAS/XMCD for 6.5 ML Co. (g) Schematic illustration of the Alq_3-Co_{top} interface in which Alq_3 and Co are represented as big blue and small yellow spots, respectively. In the magnified region, atoms such as Al, C, N, and O are shown as orange, black, blue, and red spheres, respectively.

We thank Taiwan National Center for High-performance Computing (NCHC) for providing computational resources. Ministry of Science and Technology (MOST 103-2112-M-213-007-MY3) and National Synchrotron Radiation Research Center partially funded this work.

[1] Z. H. Xiong, D. Wu, Z. V. Vardeny, and J. Shi, Giant magnetoresistance in organic spin-valve, Nature (London) **427**, 821 (2004).

[2] V. Dediu, M. Murgia, F. C. Matacotta, C. Taliani, and S. Barbanera, Room temperature spin polarized injection in organic semiconductor, Solid State Commun. **122**, 181 (2002).

[3] S. Pramanik, C. G. Stefanita, S. Patibandla, S. Bandyopadhyay, K. Garre, N. Harth, and M. Cahay, Observation of extremely long spin relaxation times in an organic nanowire spin valve, Nat. Nanotechnol. **2**, 216 (2007).

[4] A. J. Drew, J. Hoppler, L. Schulz, F. L. Pratt, P. Desai, P. Shakya, T. Kreouzis, W. P. Gillin, A. Suter, N. A. Morley, V. K. Malik, A. Dubroka, K. W. Kim, H. Bouyanfif, F. Bourqui, C. Bernhard, R. Scheuermann, G. J. Nieuwenhuys, T. Prokscha, and E. Morenzoni, Direct measurement of the electronic spin diffusion length in a fully functional organic spin valve by low-energy muon spin rotation, Nat. Mater. **8**, 109 (2009).

[5] W. J. M. Naber, S. Faez, and W. G. V. D. Wiel, Organic spintronics, J. Phys. D: Appl. Phys. **40**, R205 (2007).

[6] V. A. Dediu, L. E. Hueso, I. Bergenti, and C. Taliani, Spin routes in organic semiconductors, Nat. Mater. **8**, 707 (2009).

[7] S. Wang, Y. J. Shi, L. Lin, B. B. Chen, F. J. Yue, J. Du, H. F. Ding, F. M. Zhang, and D. Wu, Room-temperature spin valve effects in $La_{0.67}Sr_{0.33}MnO_3/Alq_3/Co$ devices, Synth. Met. **161**, 1738 (2011).

[8] C. Barraud, P. Seneor, R. Mattana, S. Fusil, K. Bouzehouane, C. Deranlot, P. Graziosi, L. Hueso, I. Bergenti, V. Dediu, F. Petroff, and A. Fert, Unravelling the role of the interface for spin injection into organic semiconductors, Nat. Phys. **6**, 615 (2010).

[9] V. Dediu, L. E. Hueso, I. Bergenti, A. Riminucci, F. Borgatti, P. Graziosi, C. Newby, F. Casoli, M. P. De Jong, C. Taliani, and Y. Zhan, Room-temperature spintronic effects in Alq_3-based hybrid devices, Phys. Rev. B **78**, 115203 (2008).

[10] X. Zhang, S. Mizukami, T. Kubota, M. Oogane, H. Naganuma, Y. Ando, and T. Miyazaki, Spin transport in $Co/Al_2O_3/Alq_3/Co$ organic spin valve, IEEE Trans. Magn. **47**, 2649 (2011).

[11] J. M. Baik, Y. Shon, S. J. Lee, Y. H. Jeong, T. W. Kang, and J. L. Lee, Electronic structure and magnetism in transition metals doped 8-hydroxy-quinoline aluminum, J. Am. Chem. Soc. **130**, 13522 (2008).

[12] F. J. Wang, Z. H. Xiong, D. Wu, J. Shi, and Z. V. Vardeny, Organic spintronics: the case of $Fe/Alq_3/Co$ spin-valve devices, Synth. Met. **155**, 172 (2005).

[13] H. Vinzelberg, J. Schumann, D. Elefant, R. B. Gangineni, J. Thomas, and B. Buchner, Low temperature tunneling magnetoresistance on (La, Sr)MnO_3/Co junctions with organic spacer layers, J. Appl. Phys. **103**, 093720 (2008).

[14] J. S. Jiang, J. E. Pearson, and S. D. Bader, Absence of spin transport in the organic semiconductor Alq_3, Phys. Rev. B **77**, 035303 (2008).

[15] W. Xu, G. J. Szulczewski, P. LeClair, I. Navarrete, R. Schad, G. Miao, H. Guo, and A. Gupta, Tunneling magnetoresistance observed in $La_{0.67}Sr_{0.33}MnO_3$/organic molecule/Co junctions, Appl. Phys. Lett. **90**, 072506 (2007).

[16] T. S. Santos, J. S. Lee, P. Migdal, I. C. Lekshmi, B. Satpati, and J. S. Moodera, Room-temperature tunnel magnetoresistance and spin-polarized tunneling through an organic semiconductor barrier, Phys. Rev. Lett. **98**, 016601 (2007).

[17] D. Sun, L. Yin, C. Sun, H. Guo, Z. Gai, X. G. Zhang, T. Z. Ward, Z. Cheng, and J. Shen, Giant magnetoresistance in organic spin valves, Phys. Rev. Lett. **104**, 236602 (2010).

[18] T. D. Nguyen, E. Ehrenfreund, and Z. V. Vardeny, Spin-polarized light-emitting diode based on an organic bipolar spin valve, Science **337**, 204 (2012).

[19] J. W. Yoo, H. W. Jang, V. N. Prigodin, C. Kao, C. B. Eom, and A. J. Epstein, Giant magnetoresistance in ferromagnet/organic semiconductor/ferromagnet heterojunctions, Phys. Rev. B **80**, 205207 (2009).

[20] Y. Q. Zhan, X. J. Liu, E. Carlegrim, F. H. Li, I. Bergenti, P. Graziosi, V. Dediu, and M. Fahlman, The role of aluminum oxide buffer layer in organic spin-valves performance, Appl. Phys. Lett. **94**, 053301 (2009).

[21] F. Borgatti, I. Bergenti, F. Bona, V. Dediu, A. Fondacaro, S. Huotari, G. Monaco, D. A. MacLaren, J. N. Chapman, and G. Panaccione, Understanding the role of tunneling barriers in organic spin valves by hard x-ray photoelectron spectroscopy, Appl. Phys. Lett. **96**, 043306 (2010).

[22] A. Riminucci, M. Prezioso, C. Pernechele, P. Graziosi, I. Bergenti, R. Cecchini, M. Calbucci, M. Solzi, and V. Dediu, Hanle effect missing in a prototypical organic spintronic device, Appl. Phys. Lett. **102**, 092407 (2013).

[23] M. Cinchetti, K. Heimer, J. P. Wustenberg, O. Andreyev, M. Bauer, S. Lach, C. Ziegler, Y. Gao, and M. Aeschlimann, Determination of spin injection and transport in a ferromagnet/organic semiconductor heterojunction by two-photon photoemission, Nat. Mater. **8**, 115 (2009).

[24] K. Ando, S. Watanabe, S. Mooser, E. Saitoh, and H. Sirringhaus, Solution-processed organic spin-charge converter, Nat. Mater. **12**, 622 (2013).

[25] Y. Q. Zhan, I. Bergenti, L. E. Hueso, V. Dediu, M. P. de Jong, and Z. S. Li, Alignment of energy levels at the $Alq_3/La_{0.7}Sr_{0.3}MnO_3$ interface for organic spintronic devices, Phys. Rev. B **76**, 045406 (2007).

[26] Y. Q. Zhan, M. P. de Jong, F. H. Li, V. Dediu, M. Fahlman, and W. R. Salaneck, Energy level alignment and chemical interaction at Alq_3/Co interfaces for organic spintronic devices, Phys. Rev. B **78**, 045208 (2008).

[27] Y. Liu, S. M. Watson, T. Lee, J. M. Gorham, H. E. Katz, J. A. Borchers, H. D. Fairbrother, and D. H. Reich, Correlation between microstructure and magnetotransport in organic semiconductor spin-valve structures, Phys. Rev. B **79**, 075312 (2009).

[28] S. Sanvito, The rise of spinterface science, Nat. Phys. **6**, 562 (2010).

[29] Y. Zhan, E. Holmstrom, R. Lizarraga, O. Eriksson, X. Liu, F. Li, E. Carlegrim, S. Stafstrom, and M. Fahlman, Efficient spin injection through exchange coupling at organic semiconductor/ferromagnet heterojunctions, Adv. Mater. **22**, 1626 (2010).

[30] L. Schulz, L. Nuccio, M. Willis, P. Desai, P. Shakya, T. Kreouzis, V. K. Malik, C. Bernhard, F. L. Pratt, N. A. Morley, A. Suter, G. J. Nieuwenhuys, T. Prokscha, E. Morenzoni, W. P. Gillin, and A. J. Drew, Engineering spin propagation across a hybrid organic/inorganic interface using a polar layer, Nat. Mater. **10**, 39 (2011).

[31] P. Ruden, Interfaces are critical, Nat. Mater. **10**, 8 (2011).

[32] S. Steil, N. Grobmann, M. Laux, A. Ruffing, D. Steil, M. Wiesenmayer, S. Mathias, O. L. A. Monti, M. Cinchetti, and M. Aeschlimann, Spin-dependent trapping of electrons at spinterfaces, Nat. Phys. **9**, 242 (2013).

[33] K. V. Raman, A. M. Kamerbeek, A. Mukherjee, N. Atodiresei, T. K. Sen, P. Lazic, V. Cacluc, R. Michel, D. Stalke, S. K. Mandal, S. Blugel, M. Munzenberg, and J. S. Moodera, Interface-engineered templates for molecular spin memory devices, Nature (London) **493**, 509 (2013).

[34] D. H. Wei, Y. L. Chan, Y. J. Hung, C. H. Wang, Y. C. Lin, Y. L. Lai, H. T. Chang, C. H. Lee, and Y. J. Hsu, Magnetic disparities at the interfaces of Co-pentacene-Co hybrid structures, Synth. Met. **161**, 581 (2011).

[35] Y. L. Chan, Y. J. Hung, C. H. Wang, Y. C. Lin, C. Y. Chiu, Y. L. Lai, H. T. Chang, C. H. Lee, Y. J. Hsu, and D. H. Wei, Magnetic response of an ultrathin cobalt film in contact with an organic pentacene layer, Phys. Rev. Lett. **104**, 177204 (2010).

[36] D. H. Wei, C. H. Wang, H. C. Chang, Y. L. Chan, C. H. Lee, and Y. J. Hsu, Direct imaging and spectral identification of the interfaces in organic semiconductor-ferromagnet heterojunction, Appl. Phys. Lett. **101**, 141605 (2012).

[37] Y. J. Hsu, Y. J. Hung, Y. C. Lin, Y. L. Lai, H. T. Chang, C. H. Wang, Y. L. Chan, C. L. Hsia, M. F. Luo, C. H. Lee, and D. H. Wei, The origin of interfacial electronic and magnetic degradation for a ferromagnet atop organic conjugated molecules, Synth. Met. **161**, 575 (2011).

[38] T. Ikegami, I. Kawayama, M. Tonouchi, S. Nakao, Y. Yamashita, and H. Tada, Planar-type spin valves based on low-molecular-weight organic materials with $La_{0.67}Sr_{0.33}MnO_3$ electrodes, Appl. Phys. Lett. **92**, 153304 (2008).

[39] H. Wang, M. F. Chiah, W. Y. Cheung, and S. P. Wong, Structure, magnetic and electrical properties of soft magnetic Co-C amorphous thin films, Phys. Lett. A **316**, 122 (2003).

[40] G. Kresse and J. Hafner, *Ab initio* molecular dynamics for liquid metals, Phys. Rev. B **47**, 558 (1993).

[41] G. Kresse and J. Hafner, *Ab initio* molecular-dynamics simulation of the liquid-metal-amorphous-semiconductor transition in germanium, Phys. Rev. B **49**, 14251 (1994).

[42] G. Kresse and J. Furthmüller, Efficient iterative schemes for *ab initio* total-energy calculations using a plane-wave basis set, Phys. Rev. B **54**, 11169 (1996).

[43] See Supplemental Material at http://link.aps.org/supplemental/10.1103/PhysRevB.91.041204 for a detailed description of DFT calculation, effectiveness of organic molecules for spin filtering in an organic spin valve: reaction-induced spin polarization for Co atop Alq_3. In addition, we provide more details about measurement techniques and further supporting experimental results.

[44] Y. P. Wang, X. F. Han, Y. N. Wu, and H. P. Cheng, Adsorption of tris(8-hydroxyquinoline)aluminum molecules on cobalt surfaces, Phys. Rev. B **85**, 144430 (2012).